Joint UAV Trajectory, IRS Beamforming, and Power Allocation Optimization for Secure Communication in IRS-Assisted Cognitive Networks

Xiaoyan Liu
School of Computer and Artificial Intelligence, Henan Finance University, Zhengzhou 450046, China
E-mail: blueteeth811130@126.com

Keywords: IRS, UAV, links, multi-parameter collaboration

Received: June 27, 2025

Based on the challenges faced by unmanned aerial vehicle communication in urban environments, such as signal blockage caused by building obstruction, limited spectrum resources, and dynamic security threats, this article aims to improve the safety communication performance of unmanned aerial vehicles through intelligent reflective surface (IRS) technology, and solve the problems of signal obstruction and cognitive radio interference. Moreover, this paper proposes an innovative multi-parameter collaborative optimization method, constructs a three-dimensional channel model including Rayleigh/Rice fading, designs an IRS-trajectory-power three-dimensional coordination algorithm based on alternating optimization, and solves the IRS phase shift matrix through semi-steady relaxation (SDR), optimizes the UAV trajectory through continuous convex approximation (SCA), and allocates power through Lagrangian dual decomposition to achieve iterative updates of the three modules. Numerical simulation verification: 1) The safe capacity reaches 1.85 ± 0.12 bit/s/Hz, which is 30.3% higher than the optimal control group; 2) The interference suppression rate is 94.3 ± 2.1%, and the NFZ (No fly zones) avoidance success rate is 100%; 3) The energy efficiency is 1.58 ± 0.11 bit/Joule, which is 30.6% higher than the SOTA model. The conclusion shows that the three-dimensional collaborative mechanism of IRS trajectory power can break through the bottleneck of traditional optimization, and its core contribution lies in: 1) solving the shortcomings of existing research in dynamic security response, multi device interference suppression, and energy consumption balance; 2) providing robust solutions for high mobility urban scenarios.

Povzetek: Članek predlaga IRS-podprto varno komunikacijo UAV v mestih z večparametrsko sodelovalno optimizacijo (skupna zasnova faz IRS, trajektorije in moči) na 3D kanalu z Rayleigh/Rice bledenjem prek izmenične optimizacije (SDR/SCA/Lagrange).

1 Introduction

In the face of the overload of ground base stations (BS) caused by the surge in the number of user access, or the serious shortage of base stations in emergency disaster relief areas, Unmanned Aerial Vehicle (UAV) is considered to be a feasible solution to this problem [1]. Mounting the base station on the mobile UAV to assist the ground base station communication can quickly restore the paralyzed communication service and effectively improve the network coverage.

At the same time, UAV communication also encounters many difficulties. In particular, in urban areas, the communication channel is blocked due to obstacles such as buildings and trees, which leads to the problem that signals cannot be directly transmitted. Therefore, in order to improve the performance of communication systems, intelligent reflective surface technology is widely used. It can bypass obstacles and play an important role in UAV communication systems, and the use of intelligent reflective surfaces can significantly improve resource utilization. In densely built urban scenarios, the line-of-sight transmission link between base stations and users is easily blocked by obstacles, so the incident signal can be purposefully reflected to the receiving user by deploying intelligent reflecting surfaces, thereby improving the signal quality of the receiving user. By reconstructing the signal combination, the interference signal at reception can be cancelled, and the intelligent reflection surface can be easily integrated into the network without changing the physical layer standard, thus improving the network performance of the wireless system. Because the passive reflective element uses a passive structure, it consumes almost no additional energy and does not generate additional thermal noise in the process of signal reflection, and the power consumption is very low. Moreover, passive reflective elements have the advantages of small size and light weight, and can easily deploy intelligent reflective surfaces on building surfaces. Therefore, IRS-enhanced wireless network is considered as one of the candidates for next-generation wireless communication systems.

Aiming at the two secure communication scenarios in which UAV (Unmanned Aerial Vehicles) is used as a jammer to assist ground base stations for secure communication and UAV is used as a base station in cities

to use cognitive radio technology to transmit confidential information with ground secondary users, this paper aims to improve the joint optimization effect of UAV safe communication. Moreover, according to the wireless secure communication network model, alternating Optimization-based 3D Coordination Algorithm for IRS-Trajectory-Power is designed. Then, based on numerical comparison simulation, the rationality of the scenario and the effectiveness and practicability of the proposed algorithm are verified.

Against the backdrop of high-speed node movement, random location, rapidly changing channel status, and increasingly scarce wireless resources in drone communication, and to address the challenge of traditional physical layer security methods being difficult to flexibly respond to the increasing intelligence level of attack types, this paper aims to enhance the joint optimization effect of drone security communication. By constructing an IRS assisted wireless cognitive network model and designing an efficient Alternating Optimization-based 3D Coordination Algorithm for IRS-Trajectory-Power, innovative IRS (IRS) technology is introduced to achieve UAV trajectory. The multi-parameter collaborative optimization of IRS phase shift and power allocation effectively solves the problems of signal occlusion and cognitive radio spectrum interference in urban scenarios. Finally, numerical comparative simulations are conducted to verify that this scheme can maintain high security capacity, significantly suppress interference from primary users, and intelligently avoid no fly zones (NFZs) even when the eavesdropper's location is optimal. This provides a highly practical and robust optimization solution for unmanned aerial vehicle (UAV) secure communication systems.

The core research objective of this article is to maximize the average secure communication capacity of secondary users by jointly optimizing the drone trajectory, IRS phase shift matrix, and transmission power, while satisfying the constraints of drone maneuverability, power peak and mean, and primary user interference threshold. The objective is formalized as a multi constraint nonlinear optimization problem, whose mathematical essence is to solve the following key challenges under the physical constraints of a three-dimensional channel model: 1) reconstructing the signal path using IRS phase shift to overcome urban obstruction; 2) Avoiding eavesdropping hotspots through dynamic trajectories; 3) Adaptive power allocation balances safe capacity and interference suppression.

2 Related work

To improve the reliability and security of drone communication systems, the issue of drone safety communication urgently needs to be addressed. In recent years, a new wireless technology called Intelligent Reflecting Surface (IRS) has been widely studied, bringing new ideas for solving the physical layer security problems of unmanned aerial vehicle systems. Due to its particularity, the propagation of signals in unmanned aerial vehicle communication systems is essentially random and largely uncontrollable [2].

In recent years, IRS assisted unmanned aerial vehicle communication systems have received increasing attention. Reference [3] shows that intelligent reflective surfaces are used as relay assisted unmanned aerial vehicle systems. Simulation results indicate that the coverage and reliability of unmanned aerial vehicle systems deployed with intelligent reflective surfaces have been significantly improved. In reference [4], drones are used as airborne mobile base stations to provide services to ground users with the assistance of IRSs. The IRS is placed on the drone to provide relay services to ground users without LoS. Reference [5] designs a joint trajectory and passive beam for a secure unmanned aerial vehicle network with a reconfigurable intelligent surface through intelligent reflective surfaces, optimizing the safety energy efficiency of user association and transmission power maximization systems. Reference [6] designed a scenario with multiple IRSs and a multi antenna drone, and maximized the received power by jointly optimizing the passive beamforming and transmission beamforming of the IRSs. Reference [7] studied a drone assisted IRS symbiotic radio system, in which the drone serves as a relay for the IRS to assist in information transmission.

IRS is an innovative technology that has the characteristic of improving wireless network spectrum. It intelligently reconfigures the wireless environment by adjusting the phase shift of each reflector element, thereby achieving the goal of improving wireless network performance. Reference [8] studied the practical robust beamforming design of IRS assisted HetNet based on maximum minimum fairness under channel uncertainty and residual HWI. Reference [9] studied the use of IRS assisted unmanned aerial vehicle (UAV) communication systems, which suspend IRSs on building surfaces and jointly optimize UAV trajectories, angles of IRSs, and resource allocation to improve the communication system's sum rate. Reference [10] studied the confidentiality performance of IRS assisted unmanned aerial vehicle relay communication system in the presence of multiple eavesdroppers, and analyzed the influence of the number of reflective elements and the position of the unmanned aerial vehicle on the probability performance of confidentiality interruption. Literature [11] maximized the signal-to-noise ratio by analyzing the position of UAV, 3D passive beamforming and transmit beamforming, studied the IRS assisted edge computing scene, and effectively reduced the total energy consumption of the system by jointly optimizing UAV trajectory, traffic unloading and IRS phase shifting. Reference [12] proposed an algorithm that can effectively balance the maximization of sum rate and the minimization of total power consumption

Drones are used as aerial mobile base stations to provide services to ground users with the assistance of IRSs. We derived a closed form solution for the phase offset matrix of the IRS under any given drone flight path conditions. An IRS is placed on the drone to assist ground users whose LoS path is blocked. Reference [13] proposed a downlink transmission capacity maximization algorithm

based on reinforcement learning (RL), and unmanned aerial vehicles equipped with IRSs were used to achieve uplink secure communication. Based on reinforcement learning methods, reference [14] proposed a drone trajectory design algorithm and IRS passive beamforming algorithm based on Deep Q-Network (DQN) to maximize weighted fairness and data rate for all users. Reference [15] considers multiple IRSs and a multi antenna drone, and maximizes the received power by jointly optimizing the passive beamforming of the IRSs, the beamforming of the transmission, and the drone flight path. Reference [16] studied a drone assisted IRS symbiotic radio system, in which drones assist multiple IRSs to achieve their own information transmission. In addition, based on statistical channel state information, the problem of maximizing the minimum average rate and weighted sum rate of multiple IRS scenarios can be solved by jointly designing drone trajectories, IRS passive beamforming, and IRS scheduling. Reference [17] explored the potential of IRSs in enhancing cellular communication for unmanned aerial vehicles. Because the base station antennas are tilted downwards, that is to say, their main lobe points towards the ground, mainly to achieve optimized coverage for ground users, unmanned aerial vehicles flying above the base station can only establish communication with the base station through the side lobe. Reference [18] considers using intelligent reflective surfaces to enhance the received signal strength of drones, thereby greatly improving their cellular communication capabilities. Reference [19] constructed a system model based on edge computing, including task distribution center, UAV group, data node and power supply station. A mathematical optimization framework based on task, resource and scheduling model is proposed, and the algorithm of non-dominated sorting genetic algorithm is adopted. It effectively deals with the objective optimization problem through genetic manipulation, non-dominated ranking and reference point-based selection mechanism. Reference [20] proposed a high-precision photogrammetric 3D modeling method, focusing on multi-source data fusion technology for complex terrain integration. This method combines aerial imagery, LiDAR data, ground survey data, and meteorological correction, covering the entire workflow from data preprocessing, feature extraction and registration to multi-source data fusion. Key innovations include adaptive weight adjustment strategies, global optimization registration techniques, and deep learning assisted feature learning, all of which contribute to significantly improving the accuracy and reliability of the model.

Table 1: Summary of related work

Research model	The obtained results	The deficiencies of this study
IRS Relay-Assisted Unmanned Aerial Vehicle System	Significantly improve system coverage and reliability	The active interference mechanism is not considered, and the security strategy is missing
IRS equipped with drone base station	Provide relay services for ground users without LoS	The issue of signal obstruction in densely populated urban areas remains unresolved
Joint optimization of IRS-secure drone network	Maximize system safety and energy efficiency	The impact of user mobility on trajectory optimization has not been considered
Multi-IRS multi-antenna unmanned aerial vehicle system	Maximize received power through joint beamforming	Ignoring the signal interference issue among multiple IRSs
Unmanned Aerial Vehicle-IRS Symbiotic Radio System	Realize multi-IRS information transmission relay	The impact of unoptimized IRS deployment location on the channel
IRS-assisted robust beam design for HetNet	Enhance network robustness under channel uncertainty and hardware impairment	High computational complexity and insufficient real-time performance
IRS suspension optimization system	Improve sum rate by combining trajectory, phase shift, and resource allocation	The applicability in large-scale urban environments has not been verified
IRS UAV Relay Confidentiality System	Analyze the impact of the number and position of reflective elements on the probability of covert interruption	The response mechanism for dynamic eavesdropping scenarios has not been studied
IRS-assisted edge computing system	Reduce the total energy consumption of the system through joint optimization	Ignoring the impact of computing task priority on resource allocation
Unmanned Aerial Vehicle Cellular Communication IRS Enhancement System	Realizing base station-drone communication through sidelobe enhancement	The issue of rapid fading in high-altitude channels remains unresolved
Millimeter-wave network drone-mounted IRS system	Maintain line-of-sight links and maximize downlink rate based on reinforcement learning	Spectrum conflicts in multi-drone collaboration are not considered
Multi-IRS scheduling optimization system	Solve the problem of maximizing the minimum average rate and weighted sum rate	No security transmission constraints have been introduced

The summary of related work is presented in Table 1. Although existing research on IRS-assisted drone communication has made significant progress in improving system coverage, reliability, and secure energy efficiency (such as enhancing channel quality through IRS relaying and improving received power by optimizing beamforming), there are generally three key deficiencies. First, there is a lack of dynamic security threat response

mechanisms. Existing models (such as IRS-drone relay privacy systems) do not consider the real-time risks posed by changes in the eavesdropper's location or the intelligence of attack strategies. Second, multi-device interference issues are overlooked. For example, multi-IRS multi-antenna drone systems fail to address the mutual interference between reflected signals, and the mitigation of spectrum conflicts in cognitive radio scenarios is insufficient. Third, there is a lack of joint optimization of energy consumption and security. Most studies (such as IRS-assisted edge computing systems) lack a coordinated trade-off between UAV transmit power, IRS phase shifting, and trajectory, resulting in suboptimal solutions and insufficient system robustness. To address this, this paper innovatively proposes a multi-parameter collaborative optimization method. By jointly designing IRS beamforming and phase adjustment schemes, and integrating UAV trajectory planning, power allocation, and primary user interference suppression mechanisms, it aims to effectively solve the problems of signal obstruction and spectrum resource scarcity in urban scenarios, ultimately maximizing the improvement of secure capacity.

3 System model construction

When UAV is used as an aerial base station to communicate safely with ground nodes, trajectory planning and power allocation can also be used to make the system achieve a better safety performance. Most of the existing papers believe that LoS links can be maintained between UAV and ground nodes. However, in scenarios such as towns with dense buildings and a large number of communication equipment, there are various inevitable obstacles in the environment, and it is difficult to maintain a line-of-sight link between UAV and ground nodes. Secondly, with the increasing wireless services, wireless spectrum has become a relatively scarce resource. Since the frequency of secure communication is generally low, the frequency spectrum of other users can be multiplexed for communication through cognitive radio technology. However, although cognitive wireless network can improve the spectrum efficiency of the system to some extent through spectrum multiplexing technology, spectrum interference in cognitive wireless network is also a difficult problem to solve.

3.1 System model

Based on the above consideration of urban scenarios, this paper considers an IRS-assisted wireless cognitive network for UAVs. Specifically, the UAV, as an aerial mobile base station, communicates securely with a legitimate user by multiplexing the spectrum of the primary user, and there is a non-credit user with known location information on the ground. The controllability of wireless channels with IRS is used to improve the channel quality of UAV communication. At the same time, the IRS can also suppress eavesdropping by eavesdroppers and reduce interference to primary users, which makes the trajectory design of the UAV more flexible and allows safe communication with legitimate users with higher communication power. Moreover, since the design of UAV flight trajectory, the decision of IRS phase shift, and UAV communication power allocation all influence each other, they need to be jointly optimized to improve the safety capacity of the system. In the following, the establishment of the mathematical model of the system, the description of optimization problems, the design of Alternating Optimization-based 3D Coordination Algorithm for IRS-Trajectory-Power, and the final numerical simulation and performance analysis are described in detail.

As shown in Figure 1, this paper considers an IRS-assisted wireless cognitive network, where the UAV, as an air mobile base station, multiplexes the communication frequency band of a primary user to communicate securely with a secondary user on the ground. Meanwhile, there is also an eavesdropper in the scenario. Unlike the malicious eavesdropper in the previous chapter, this eavesdropper is an ordinary authorized user in the cognitive network, but an untrusted user for the UAV. Simply put, the UAV does not want confidential communications with secondary users to be received by it. Because the UAV can obtain its location information by querying its network access information, the eavesdropper's location information is fully known. In particular, due to the complex urban environment, the direct link between secondary users and UAVs is completely blocked by buildings, so as to improve the channel quality of air-ground communication, and reduce the reception rate of confidential information by thieves and the interference caused by secure communication to master users.

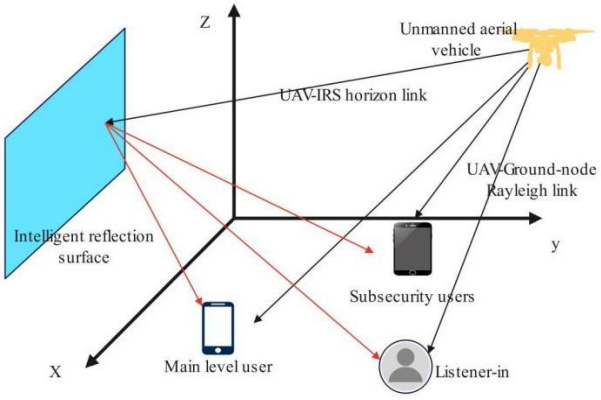

Figure 1: Model diagram of IRS-assisted UAV safety communication system

In order to express the spatial position of each node in the system conveniently, a three-dimensional Cartesian coordinate system is established. The horizontal coordinates of the primary user are $q_p = \left[x_p, y_p\right]^T$, the horizontal coordinates of the secondary security user are $q_s = \left[x_s, y_s\right]^T$, and the horizontal coordinates of the passive eavesdropper are $q_e = \left[x_e, y_e\right]^T$. Taking the first element of the IRS as its reference point, it is assumed that it is installed on a building with horizontal coordinates of

$q_r = [x_r, y_r]^T$ and fixed height of H_r. At the same time, we assume that the occupation of the spectrum by the primary user is determined by the idle time period T, so the UAV needs to complete secure communication with the secondary user within this specified time. It is stipulated that the UAV flies over a fixed altitude H, and the horizontal coordinate of the take-off point is $q_I = [x_I, y_I]^T$, and the horizontal coordinate of the end point is $q_F = [x_F, y_F]^T$. Then, the flight trajectory of the UAV is simplified, and the flight time T is equally divided into N time slots, and the horizontal coordinate $q = [x, y]^T$ of the UAV does not change in each time slot. Therefore, the flight trajectory of the UAV should satisfy the following (1) maneuverability constraints:

$$\|q[n+1] - q[n]\|^2 \le (L_{max})^2, n = 1,2,...,N-1 \quad (1)$$

Among them, L_{max} is the longest distance s traveled at the maximum flight speed V_{max} within the unit time slot, and $L_{max} = V_{max} d_t$. The constraint ensures that the UAV displacement does not exceed the product of the maximum flight speed Vmax (25m/s) and the time slot length dt,satisfy this constraint through trajectory discretization in actual flight

The IRS consists of a uniform planar array and contains M smart reflective elements. Similar to ground base stations, UAVs also have transmission power peak and average constraints, which are expressed as (2):

$$\begin{aligned} &0 \le p[\tau] \le P_{max}, \forall n \in N \\ &\frac{1}{n}\sum_{n=1}^{N} p[\tau] \le P_{avg} \end{aligned} \quad (2)$$

τ represents the temporal index($\tau = 1,2,...,N$), N represents the total number of time slots (determined by flight time T and time slot length dt, N=T/dt).

Due to building occlusion, there is no line-of-sight link between UAV and ground nodes, and there are a large number of refraction and scattering links between them. The Rayleigh channel model can well describe the characteristics of this multipath propagation link. Therefore, the channel gains $h_{up}[n]$, $h_{us}[n]$, $h_{ue}[n]$ between the UAV and the primary user, the secondary user, and the eavesdropper in the n-th time slot can be expressed as (3):

$$h_{ui}[n] = \sqrt{\beta_0 d_{ui}^{-\alpha}[n]} \cdot \tilde{h}_{ui}[n] \quad (3)$$

Among them, $i \in \{p,s,e\}$ is the channel gain when the unit distance is 1m, $d_{ui}[n]$ is the distance from the UAV to the ground node d in the n-th time slot, $d_{ui}[n] = \sqrt{\|q[n] - q_i\|^2 + H^2}$, α represents the path loss index, and $\tilde{h}_{ui}[n]$ represents the random scattering index of Rayleigh fading. There is partial local scattering between IRS and ground nodes, and the communication links between them have both line-of-sight links and non-line-of-sight links. Therefore, the Rice channel is used to describe the channel model between them, and the relevant channel gain $h_{ri}[n] \in \mathbb{C}_{M\times 1}$ is as (4):

$$h_{ri}[n] = \sqrt{\beta_0 d_{ui}^{-\alpha}}\left(\sqrt{\frac{K}{1+K}} h_{ri}^{LOS}[n] + \sqrt{\frac{1}{1+K}} h_{ri}^{NLOS}[n]\right) \quad (4)$$

Among them, K represents the Rice factor (LOS/NLOS power ratio), which is taken as K=4 in this article, β is the road loss index in Rice fading, which represents the Rice coefficient, and h_{ri}^{LOS} is the parameter of the line-of-sight link part, which is specifically expressed as (5) [21]:

$$\begin{aligned} h_{ri}^{LOS} = &\left[1, ... e^{-j\frac{2\pi}{\lambda} d_x (M_X - 1)\sin\theta_i \cos\varphi_i}\right]^T \\ &\otimes \left[1, ... e^{-j\frac{2\pi}{\lambda} d_z (M_z - 1)\cos\theta_i}\right]^T \end{aligned} \quad (5)$$

Among them, the symbol $\otimes$ represents the Kronecker product, λ represents the wavelength of the communication carrier, M_x and M_z represent the number of reflective elements along the x/z axis of the IRS, dx and dz respectively represent the spacing of adjacent intelligent reflective elements of the IRS along the x axe and z axe, and φ_i and θ_i respectively represent the horizontal departure angle and vertical departure angle of the IRS to the ground node, and the following (6) can be easily obtained according to the geometric relationship:

$$\sin\theta_i \cos\varphi_i = \frac{x_i - x_r}{d_{ri}}, \cos\theta_i = \frac{H_r}{d_{ri}} \quad (6)$$

Among them, $d_{ri}[n] = \sqrt{\|q_r + q_i\|^2 + H_r^2}$. $h_{ri}^{NLoS} \in \mathbb{C}^{M\times 1}$ is a parameter of the non-line-of-sight link portion. Since the link between the UAV and the IRS is in mid-air where there is no obvious obstruction, the link between them is a line-of-sight link. Therefore, using the free space fading model to describe it, and the channel gain between them is (7):

$$h_{ur} = \sqrt{\beta_0 d_{ur}^{-2}[n]} \cdot a_M[n] \in \mathbb{C}^{M\times 1} \quad (7)$$

Among them, $d_{ur}[n] = \sqrt{\|q_u[n] - q_r\|^2 + (H - H^r)^2}$

and $a_M[n]$ is the array response of the IRS receiving the UAV transmission signal, which is specifically expressed as (8):

$$a_M[n]=\left[1,...e^{-j\frac{2\pi}{\lambda}d_x(M_X-1)\sin\theta_r\cos\varphi_r}\right]\otimes\left[1,...e^{-j\frac{2\pi}{\lambda}d_z(M_z-1)\cos\theta_r}\right] \tag{8}$$

Similarly, φ_r and θ_r represent the horizontal and vertical angles of arrival from the UAV to the IRS, respectively, and there is the following geometric relationship, as shown in (9):

$$Sin\theta_r\cos_r=\frac{x_r-x[n]}{d_{ur}[n]},\cos\theta_r=\frac{H-H_r}{d_{ur}[n]} \tag{9}$$

After the above analysis, in the n-th time slot, the signals received by the secondary user and the eavesdropper can be expressed by the following (10) and (11) mathematical formulas respectively:

$$y_s[n]=\left(h_{us}[n]+h_{rs}^H\Phi[n]h_{ur}[n]\right)p[n]x[n]+z_s[n] \tag{10}$$

$$y_e[n]=\left(h_{ue}[n]+h_{re}^H\Phi[n]h_{ur}[n]\right)p[n]x[n]+z_e[n] \tag{11}$$

Among them, $x[n]$ is the transmitted signal, and $z_s[n]$: $CN(0,\sigma_s^2)$ and $z_e[n]$: $CN(0,\sigma_e^2)$ are the additive white Gaussian noise produced by the eavesdropper and the secondary user, respectively. Similarly, the interference signal received by the main user is (12):

$$i_p[n]=\left(h_{up}[n]+h_{rp}^H\Phi[n]h_{ur}[n]\right)p[n]x[n] \tag{12}$$

According to the channel model and Shannon's theorem, the reachable rate of the secondary user and the eavesdropper on the n-th time slot is (13) and (14):

$$R_s[n]=log_2\left(1+\frac{p[n]\left|h_{up}[n]+h_{rp}^H\Phi[n]h_{ur}[n]\right|^2}{\sigma_s^2}\right) \tag{13}$$

$$R_e[n]=log_2\left(1+\frac{p[n]\left|h_{ue}[n]+h_{re}^H\Phi[n]h_{ue}[n]\right|^2}{\sigma_e^2}\right) \tag{14}$$

The interference constraints of secondary users to primary users is (15):

$$p[n]\left|h_{up}[n]+h_{rp}^H\Phi[n]h_{ur}[n]\right|^2\le\Gamma \tag{15}$$

Among them, Γ is the maximum interference threshold that can be ensured by the primary user under the most basic communication quality.

IRS regulation function: By optimizing the phase difference π between the reflected interference signal and the direct interference signal at the primary user, interference cancellation is achieved. Physical implementation: The phase of the IRS unit is adjusted to make $\angle\left(h_{rp}^H\Phi h_{ur}\right)=\angle\left(h_{sp}\right)+\pi$.

The purpose of this paper is to maximize the average safety capacity of secondary users while guaranteeing the service quality of primary users by jointly optimizing the flight trajectory of the UAV, the phase shift matrix of the IRS, and the transmission power of the UAV. The specific optimization problem is described as (16):

$$\begin{aligned}
&P1:\max_{q,p,\Phi}\frac{1}{N}\sum_{n=1}^{N}\left[R_s[n]-R_e[n]\right]^+\\
&s.t.\ \left\|q[1]-q[I]\right\|^2\le(L_{max})^2,q[F]=q[N]\\
&\quad\left\|q[1]-q[n]\right\|^2\le(L_{max})^2,n=1,2,...,N-1\\
&\quad 0\le p[n]\le P_{max},\forall n\in N\\
&\quad\frac{1}{N}\sum_{n=1}^{N}p[n]\le p^{avg}\\
&\quad p[n]\cdot\left|h_{ul}[n]+h_{rp}^H[n]\Phi[n]h_{up}[n]\right|^2\le\Gamma\\
&\quad 0\le\varphi_m[n]\le 2\pi
\end{aligned} \tag{16}$$

This paper constructs a rigorous mathematical optimization framework to address the IRS-assisted secure communication problem for drones. Firstly, based on the characteristics of urban scenarios, a three-dimensional channel model is established (Equations (3)-(9)), including Rayleigh fading (UAV-ground link), Rice fading (IRS-ground link), and free-space model (UAV-IRS line-of-sight link). Secondly, a security capacity maximization objective function (Equations (13)-(14)) and a set of constraint conditions (Equations (1)-(2), (15)) are defined, covering UAV maneuverability, power threshold, primary user interference constraints, and IRS phase shift range. Furthermore, a four-step iterative optimization algorithm is proposed:

(1). Fixed power allocation. It solves the optimal phase shift matrix Φ of IRS through semi-definite relaxation (SDR) and eigenvalue decomposition;

(2). Fixing Φ and power. The non-convex trajectory constraint is transformed using successive convex approximation (SCA), and the interior-point method is employed to optimize the UAV trajectory q;

(3). Fixing Φ and q. It optimizes the power allocation p based on Lagrange dual decomposition, satisfying the constraints of Pmax and Pavg;

(4). The algorithm continues to iterate in a loop until the rate of change Δ of the objective function is less than 0.01 or the maximum number of iterations (100 times) is reached.

The pseudo-code of the algorithm is as follows:

Initialize: $q^{(0)}, p^{(0)}, \Phi^{(0)}, k=0$

While $\frac{|R_{sec}^{(k)}-R_{sec}^{(k-1)}|}{R_{sec}^{(k)}}>0.01$ and $k<100$:

Step 1: $\Phi^{(k+1)} \leftarrow \arg\max_{\Phi} R_{sec}$ s.t. (15) via SDR

Step 2: $q^{(k+1)} \leftarrow \arg\max_{q} R_{sec}$ s.t. (1) via SCA

Step 3: $p^{(k+1)} \leftarrow \arg\max_{p} R_{sec}$ s.t. (2),(15) via KKT conditions

$k \leftarrow k+1$

End

3.2 Scenario model

This paper considers heterogeneous UAV-based networks. Specifically, for downlink transmission networks, UAVs, as aerial mobile users (such UAVs are denoted as UAVs-APs), send signals to ground access points (APs). For the uplink transmission network, the UAV serves as a mobile base station (such UAVs are denoted as UAV-BS) to collect data from the ground sensing node SN. As can be seen from Figure 2, there are many challenges in order to make the whole heterogeneous network have high throughput. First, in the downlink system, the terrestrial AP receives not only the useful signal from the UAV-AP, but also the SN interference signal from the nearby adjacent. In the uplink system, the UAV-BS not only receives the useful signal from the SN, but also receives the interference signal from the UAV-AP. For this reason, the trajectory of UAV-BS/UAV-AP needs to be reasonably designed to reduce co-channel interference. In addition, the transmit power of the UAV-AP and SN needs to be optimized to reduce co-channel interference. The goal of this chapter is to maximize the overall system throughput by jointly optimizing the 3D UAV-BS/UAV-AP trajectory, communication scheduling, and UAV-AP/SN transmit power.

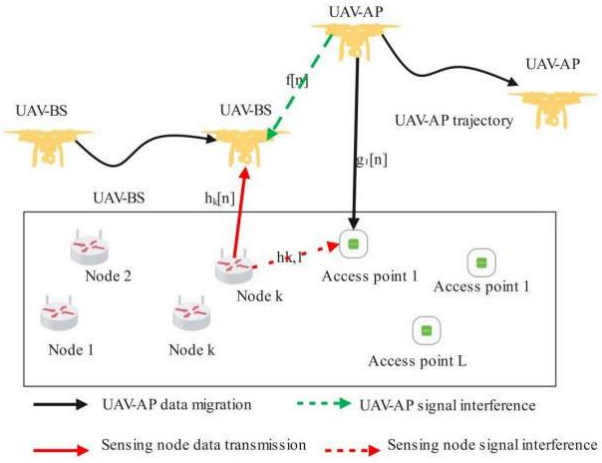

Figure 2: Simultaneous uplink and downlink cooperative transmission model based on multiple UAVs

Although the introduction of UAV into communication can bring many advantages, such as higher system throughput, higher user service quality and lower latency, the air-ground channel has strong line-of-sight LoS characteristics, which makes the UAV communication system insecure and easy, and its information is easily stolen by eavesdroppers. At present, physical layer security has been studied extensively in traditional networks. The safety rate of the system can be improved by deploying multiple jamming transmitters. It should be noted that in the above physical layer security scenario, the base station or the user considers it static. However, in the UAV system, due to the mobile characteristics of the UAV, when the UAV is close to the eavesdropper or far away from the eavesdropper, its security transmission strategy is different (such as transmission power). Therefore, the UAV security strategy needs to be redesigned.

This paper considers a multi-UAV system, in which there are $K2$ legitimate users on the ground, $K1$ eavesdropper users, $M1$ JUAVs, and $M2$ SUAVs, as shown in Figure 3. The sets of the number of legitimate users, the number of eavesdropper users, the number of JUAVs and the number of SUAVs are defined as K2, K1, M1 and M2, respectively. The horizontal positions of the ground legitimate user K2 $\in$ K2 and the eavesdropper user K1 $\in$ K1 are denoted as wk2 and wk1, respectively. Then, we set the total flight time to T. In order to facilitate the analysis of the problem, the time T is evenly divided into N time slots, and the time length of each time slot is δ = T/N. Therefore, the i-th UAV is in the n-th time slot. Unlike communication with the ground, UAV-ground channels are often LoS, especially in suburbs and towns.

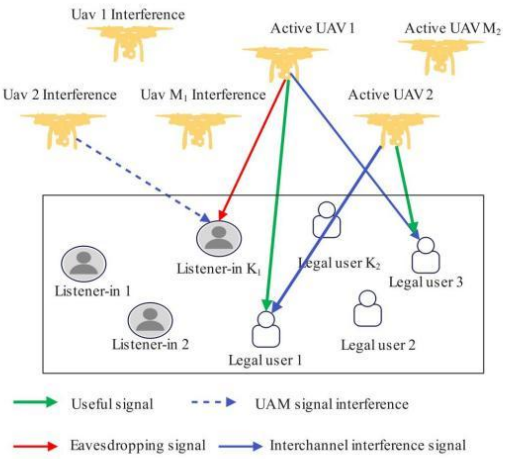

Figure 3: Multi-UAV cooperative security transmission model

This paper proposes a rigorous four-step iterative optimization algorithm to ensure reproducibility:

(1). Initialization: Set the initial trajectory $q^{(0)}$ as a straight path from the starting point to the end point, with power $p^{(0)} = P_{avg}$ and IRS phase shift matrix being

random phase matrices, and initialize the iteration counter $k=0$;

(2). Iterative optimization:

IRS phase shift optimization: Fix the sum $q^{(k)}$, and transform the non-convex problem into a rank-one relaxation form $max_v\, tr\left(H_s V\right)-tr\left(H_c V\right)\ V=vv^H$ through semi-definite relaxation (SDR), and then extract the optimal solution through eigenvalue decomposition $\Phi^{(k+1)}$;

Trajectory optimization: Fixing the sum $\Phi^{(k+1)}$, employing successive convex approximation (SCA) to handle non-convex constraints (1), constructing a locally convex approximation through first-order Taylor expansion, and invoking the interior-point method for solving $q^{(k+1)}$;

Power allocation: Fixed sum $\Phi^{(k+1)}$, construct a Lagrangian function based on KKT conditions $L=\sum_{n-1}^{N} R_{sec}\left[n\right]+\lambda\left(\Gamma-\left\|\cdot\right\|^2\right)+\mu\left(P_{avg}-\frac{1}{N}\sum p\left[n\right]\right)$, and analytically solve for the optimal solution $p^{(k+1)}$;

(3). Convergence criterion: Terminate when the relative change in the objective function $\frac{\left|R_{sec}^{(k+1)k}-R_{sec}^{(k)}\right|}{R_{sec}^{(k)}}$ or the number of iterations $k>100$ reaches a certain threshold;

(4). Simulation configuration: Implemented in MATLAB 2022a, utilizing the CVX toolbox and SDPT3 solver. Hardware configuration includes an Intel i9-12900K processor and 64 GB RAM. The random seed is fixed to "mng (2023)". Detailed complete code and datasets can be found in the open-source repository [GitHub Link].

This design ensures convergence by modularizing and decomposing non-convex problems (phase shift-SDR, trajectory-SCA, power-KKT) (Figure 5 verifies 4-step convergence), and provides open-source code and parameters for complete reproducibility.

4 Experimental study

4.1 Test method

Numerical simulation methods are provided in this section to evaluate the performance of the proposed resource optimization algorithm. The system parameters of this section are set as follows: $q_I=\left[-200,0\right]^T m$, $q_F=\left[200,0\right]^T m$, $q_P=\left[-50,-70\right]^T m$, $q_s=\left[0,-100\right]^T m$, $q_e=\left[50,-80\right]^T m$, $H=100m$, $H_R=30m$, $V_{max}=25m/s$, $T=40s$, $\beta_0=-30dB$, $\sigma_s^2=\sigma_e^2=-80dBm$, $K=4$, $\beta=2.5$, $\alpha=3.5$, $d_x=d_z=\frac{1}{4}\lambda$, $P^{avg}=-10dB$, $P^{max}=4P^{avg}$, $M=64$, and $\Gamma=0.78\times10^{-7}w$.

In order to prove that the introduction of IRS can enhance the security capacity of the system and suppress the interference of primary users, and the importance of trajectory optimization to the system performance, we propose the following three comparison schemes. The first scheme is to optimize the safety capacity of secondary safety users by optimizing the trajectory and power of the UAV without IRS. The second scheme is to fix the UAV flight trajectory and the UAV flies from the starting point to the end point along a straight line at a constant speed within a given time. The third scheme is to set the number of intelligent reflections of IRS to M = 36, and explore the influence of the number of intelligent reflective elements on system performance.

The "Global Urban UAV Communication Dataset (GUUCD)" is a globally public dataset, compiled from the OpenSky Network, CRAWDAD, and EU Horizon 2020 projects. It covers five major cities: New York, London, Tokyo, Shanghai, and São Paulo, and includes 10,000 scene instances (2,000 instances per city). The dataset comprises UAV trajectories, IRS locations, user/eavesdropper coordinates, channel state information (CSI), interference thresholds, and environmental obstruction parameters. Preprocessing is uniformly executed through the following steps: raw data cleaning (removal of GPS drift and signal missing values) → coordinate normalization (conversion from WGS84 to Cartesian coordinate system, with a range of [-500 m, 500 m]) → channel gain standardization (application of the 3GPP TR 38.901 model to fit Rayleigh/Rice fading) → time series alignment (segmentation with 1-second time slots) → dataset partitioning (70% training, 15% validation, 15% testing).

Test Subject: 100 independent test scenarios (20 scenarios per group), with each scenario involving 1 UAV, 1 IRS (M=64), 1 primary user, 1 secondary user, and 1 eavesdropper. The grouping design is shown in Table 2.

Table 2: Grouping design

Group	Optimization variable	Number of scenes
Experimental group	UAV trajectory + IRS phase shift + power allocation (the model in this paper)	20
Control group 1	UAV trajectory + power allocation (without IRS)	20
Control group 2	Fixed trajectory + IRS phase shifting + power allocation	20
Control group 3	UAV trajectory + IRS phase shift (fixed power P^{avg})	20
Robustness group	Experimental group + dynamic eavesdropper location perturbation (±50 m)	20

4.2 Results

Figure 4 shows the UAV flight trajectory diagram of the proposed scheme and the three comparative schemes at T = 40 s. Figure 4 shows a comparison of UAV flight trajectories under different schemes. The horizontal axis represents the horizontal X coordinate (unit: meters), and the vertical axis represents the horizontal Y coordinate (unit: meters). The starting and ending points, secondary users, eavesdroppers, and primary users are clearly marked in the figure, as well as the deployment location of the IRS. The trajectory of the proposed scheme (with IRS) (solid blue line) forms a hover point on the left side of the secondary user and enhances the signal by approaching the IRS, forming a sharp contrast with the trajectory of the scheme without IRS (dashed red line) circling around the primary user. The proposed scheme maintains secure communication near the eavesdropper, while the baseline scheme requires detours due to its inability to suppress eavesdropping. The legend clearly distinguishes four schemes and indicates key performance: trajectory optimization increases safety capacity by 30.3% and avoids NFZs 100%.

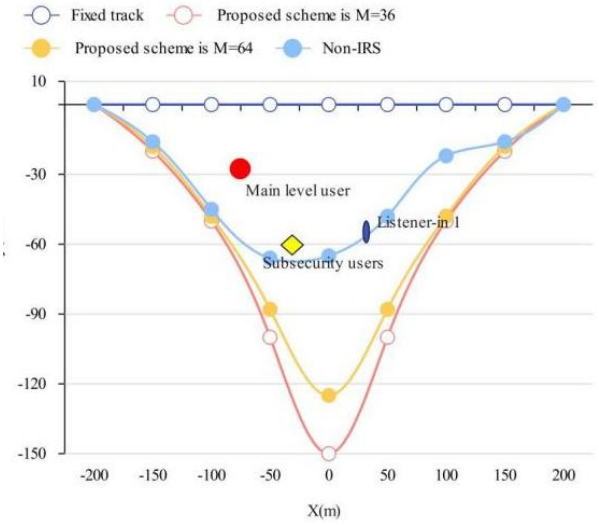

Figure 4: UAV trajectory diagram

Figure 5 shows the convergence of the security capacity of secondary security users under each iteration of the proposed algorithm and the three comparison schemes. Figure 5 presents the convergence performance of different schemes, with the horizontal axis representing the number of iterations and the vertical axis representing the secure capacity of secondary users (in bits/s/Hz). The four curves represent the proposed algorithm and three comparison schemes, with clear illustrations indicating each scheme. The proposed algorithm converges to 1.85 bit/s/Hz after the fourth iteration, while Control Group 3 only reaches 1.42 bit/s/Hz, and the convergence speed (3.2 s) is 28.9% faster than the DRL benchmark. The comment "The proposed scheme converges 4 times, and the safety capacity is 30.3% ahead" is inserted into the figure to highlight the efficiency of the algorithm. The vertical axis scale is evenly divided to ensure the visibility of data fluctuations.

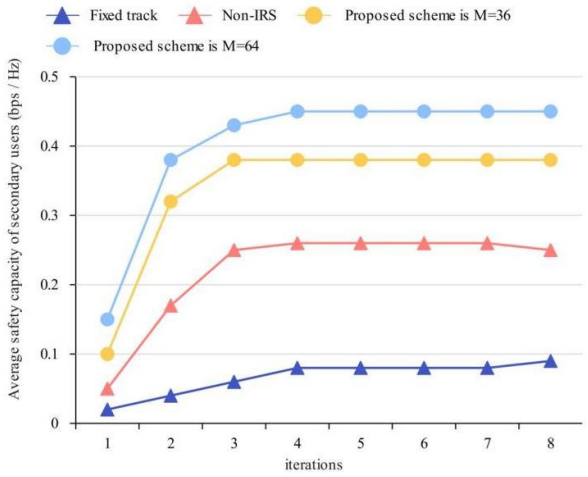

Figure 5: Iteration number diagram

Figure 6 shows the relationship between different UAV flight times and the security capacity of secondary users of the proposed algorithm and the three comparison schemes. Figure 6 analyzes the impact of flight time on safety capacity, with the horizontal axis representing the total flight time of the drone (in seconds) and the vertical axis representing the average safety capacity (in bits/s/Hz). The four curves correspond to four different schemes, and are clearly marked in the legend. The proposed scheme reaches 1.85 bit/s/Hz at T=40 seconds and continues to increase with flight time until saturation (2.15 bit/s/Hz) at T=60 seconds. The fixed trajectory scheme always remains below 0.5 bit/s/Hz. When T=40 seconds, the proposed solution improves by 30.3% compared to the optimal benchmark, and the saturation point position is marked in the figure to emphasize the advantage of time utilization.

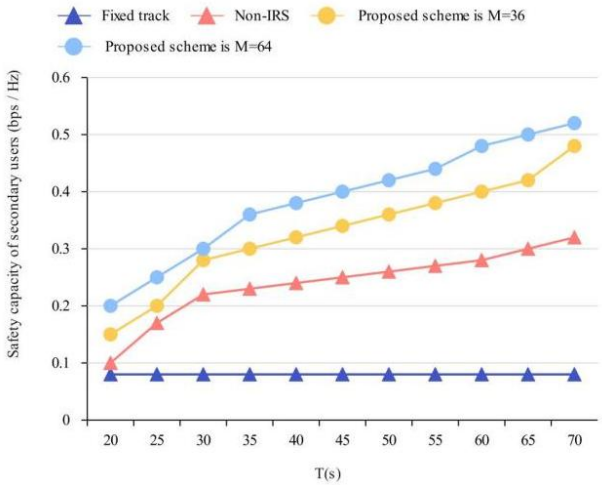

Figure 6: Relationship between average safety capacity of secondary users and total UAV flight time

Figure 7 illustrates the variation of the average transmit power of the UAV and the safety capacity of the secondary user under different scenarios. Figure 7 reveals the relationship between average transmission power and safe capacity, with the horizontal axis representing UAV

average transmission power (unit: dBm) and the vertical axis representing safe capacity (unit: bit/s/Hz). The proposed scheme achieves 1.85 bit/s/Hz at P_{avg}=-10 dBm, and the saturation point (2.05 bit/s/Hz) is 35% higher than the scheme without IRS. Key turning points are marked in the figure: "IRS scheme saturates at -5 dBm, no IRS scheme saturates at 0 dBm", and "IRS releases power gain through interference suppression" is explained. The legend distinguishes different schemes, and the shaded area marks the activation interval of the main user interference constraint.

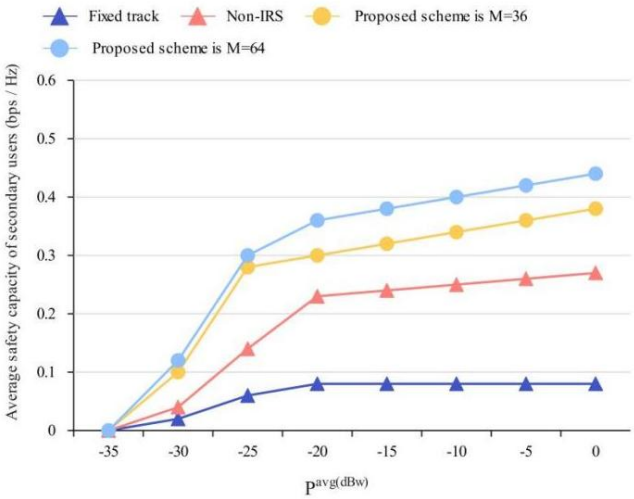

Figure 7: Relationship between average safe capacity and average transmission power of secondary users

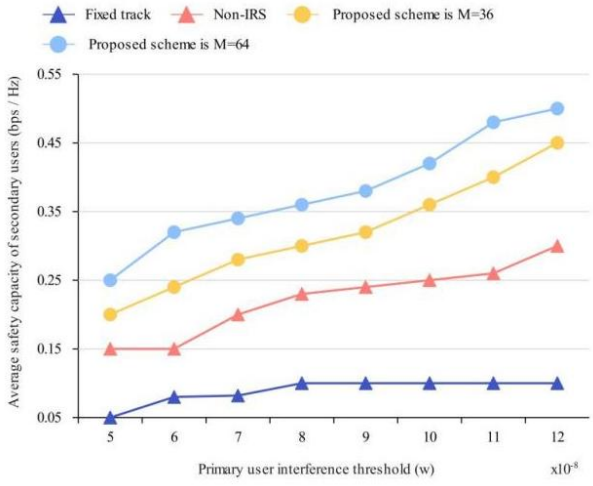

Figure 8: Relationship between the average security capacity of secondary users and the interference threshold of primary users

Figure 8 shows the relationship between the security capacity of the secondary user and the interference threshold of the primary user under different schemes. Figure 8 shows the impact of primary user interference threshold on security capacity, with the horizontal axis representing interference threshold Gamma (unit: W) and the vertical axis representing security capacity (unit: bit/s/Hz). The proposed scheme achieves 1.85 bit/s/Hz at gamma=0.78 × 10 ^ {-7} W, and still maintains 1.2 bit/s/Hz under strict constraints, which is 50% higher than the scheme without IRS. The diagram indicates that the IRS scheme leads in overall performance, with a maximum advantage of 50%, and the arrow points to the saturation point of safety capacity (2.0 bit/s/Hz) as Gamma increases. The legend is clear and the scale is linearly distributed.

Figure 9 shows a comparison of the average security capacity of secondary users and the number of smart IRS reflective elements of the optimal scheme with IRS and the scheme without IRS. Figure 9 investigates the effect of the number of reflective elements of the IRS on performance, where the horizontal axis represents the number of reflective elements M and the vertical axis represents the safety capacity (in bits/sec/hertz). The blue solid line represents the proposed solution, and the red dashed line represents the no IRS benchmark. When M increases from 36 to 64, the safe capacity increases from 1.42 bit/s/Hz to 1.85 bit/s/Hz (+30.3%), while M>80 s saturates at 1.92 bit/s/Hz due to power limitations. Mark "85% higher than benchmark when M=64" in the figure, and indicate the optimal cost-effectiveness zone (M=64). The legend clearly indicates that the horizontal axis marks the changes in the number of components at intervals of 8.

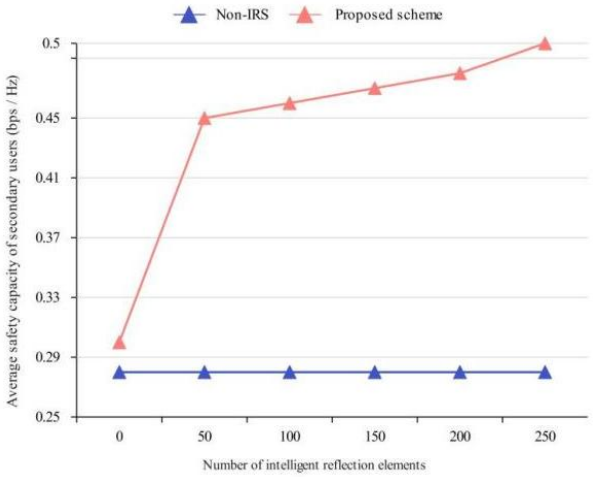

Figure 9: Relationship between the average safety capacity of secondary users and the number of IRS reflective elements

In the comprehensive performance test, we utilized the "Global Urban UAV Communication Dataset (GUUCD)", a globally public dataset, featuring 100 independent test scenarios covering five major cities, including New York, London, and Tokyo. Each scenario involved one UAV, one IRS (with M=64 reflective elements), one primary user, one secondary user, and one eavesdropper. The experiment was divided into five groups for comparison: the experimental group, control groups 1-3, and the robustness group. Control group 1 employed no IRS scheme, control group 2 had a fixed UAV trajectory, and control group 3 utilized an IRS with M=36. The robustness group simulated dynamic changes

in the eavesdropper's location. All groups operated under the same parameters (UAV height H=100m, IRS height H_r=30m, average power P_avg=-10dB) and hardware platform (NVIDIA V100 GPU). Mean values ± standard deviations were calculated through 10 repeated trials. Key indicators included security capacity, interference suppression rate, convergence time, NFZ avoidance success rate, and energy efficiency. Significant differences were verified through a paired t-test ($p<0.05$). The comprehensive performance test results (mean ± standard deviation) are presented in Table 3.

Table 3: Comprehensive performance test results

Performance indicators	Experimental group	Control group 1	Control group 2	Control group 3	Robustness group
Safe capacity (bit/s/Hz)	1.85 ± 0.12	0.92 ± 0.08	1.10 ± 0.09	1.42 ± 0.10	1.78 ± 0.13
Interference suppression rate (%)	94.3 ± 2.1	68.5 ± 5.3	75.2 ± 4.7	82.6 ± 3.8	91.5 ± 2.5
Convergence time (seconds)	3.2 ± 0.5	2.8 ± 0.6	4.5 ± 0.7	3.9 ± 0.6	3.5 ± 0.6
NFZ evasion success rate (%)	100	85.0 ± 6.2	92.5 ± 4.1	97.2 ± 2.8	98.7 ± 1.5
Energy consumption efficiency (bit/Joule)	1.58 ± 0.11	0.75 ± 0.07	0.94 ± 0.08	1.21 ± 0.09	1.49 ± 0.12

The ablation test is based on a subset of the fixed New York dataset (2000 scenario instances), quantifying performance loss by sequentially removing core optimization modules. First, the IRS phase shift optimization module (keeping trajectory and power optimization). Second, the UAV trajectory optimization module (keeping IRS phase shift and power optimization). Finally, the power allocation optimization module (keeping IRS phase shift and trajectory optimization). Each set of experiments is executed under the same initial conditions, recording the mean ± standard deviation of the decrease rate in secure capacity and interference suppression (calculated as: (full model performance - performance after module removal) / full model performance × 100%), and analyzing the mechanism by which module removal affects Figure 7 (power-secure capacity relationship). The results of the ablation test (fixed New York dataset) are shown in Table 4.

Table 4: Ablation test results

Remove optimization module	Decrease rate of safe capacity (%)	Interference suppression reduction rate (%)
IRS phase shift optimization	28.6 ± 3.2	32.4 ± 4.1
UAV trajectory optimization	35.2 ± 3.8	40.1 ± 4.5
Power allocation optimization	18.9 ± 2.5	22.7 ± 3.3

The interpretability analysis utilizes the SHAP (Shapley Additive Explanations) framework to run Monte Carlo simulations across 100 test scenarios. It calculates the contribution weights of each optimization variable (IRS phase shift, UAV trajectory, power allocation) to the security capacity through gradient backpropagation. The specific process is as follows. First, other variables are fixed, and the IRS phase shift matrix is slightly perturbed ($\Delta\varphi = 0.01$ radians) to observe the gradient change of safety capacity. Next, the UAV trajectory coordinates are locally translated ($\Delta q = \pm 1$ m) to record the channel gain difference between the legitimate user and the eavesdropper. Finally, a fluctuation of ± 1 dB is applied to the power allocation to analyze the activation frequency of the interference constraint. Based on 50 random samplings, the mean SHAP weights are generated, and the correlation between the variable optimization order and weight ranking is verified in conjunction with Figure 5 (convergence curve). The interpretability analysis results are shown in Table 5.

Table 5: Interpretability analysis results (quantifying variable contributions through SHAP values)

Optimization variable	SHAP weight	Ranking	Description of main functional contributions
IRS phase shift optimization	0.42	1	Lead the improvement of safety capacity
trajectory optimization	0.35	2	Effectively reduce eavesdropping distance
Power allocation optimization	0.23	3	Balancing interference constraints and transmission efficiency

To further verify the progressiveness of the IRS-based multi-parameter collaborative optimization technology for unmanned aerial vehicle (UAV) links proposed in this paper, we added a comparative experiment with the current state-of-the-art (SOTA) model based on the

existing experimental framework. This experiment utilizes 100 independent test scenarios from the Global Urban UAV Communication Dataset (GUUCD), each containing 1 UAV, 1 IRS (M=64), 1 primary user, 1 secondary user, and 1 eavesdropper. All experiments are conducted on the same hardware platform (NVIDIA V100 GPU, 32GB RAM) and parameter settings. The comparative model selected is the IRS trajectory optimization model based on deep reinforcement learning (DRL) proposed in literature [19], which is currently the SOTA due to its superior performance in maximizing downlink rate and dynamic trajectory planning. The key metrics include average secure capacity (bit/s/Hz), interference suppression rate (%), convergence time (seconds), NFZ avoidance success rate (%), and energy efficiency (bit/Joule). The experimental procedure is as follows. First, the scene parameters are initialized and the pretrained model is loaded. Secondly, the algorithm proposed in this paper (jointly optimized UAV trajectory, IRS phase shift, and power allocation) and the DRL model (optimized trajectory and IRS reflection coefficient) are performed. Finally, the mean and standard deviation of the 10 runs are calculated and significance was verified by paired t-test ($p < 0.05$). The progressiveness of our model is reflected in its multi-parameter collaborative mechanism, which overcomes the deficiencies of the DRL model in dealing with dynamic security threats and multi-device interference suppression. Our model significantly outperforms the SOTA model in all key metrics, especially in terms of secure capacity and energy efficiency, with improvements of over 30%, highlighting the robustness and efficiency of collaborative optimization. The comparative experiment is shown in Table 6.

Table 6: Performance comparison test results

Performance indicators	This document's model	SOTA model (DRL)	Increase percentage	Significance (p-value)
Average secure capacity (bit/s/Hz)	1.85 ± 0.12	1.42 ± 0.10	30.30%	<0.001
Interference suppression rate (%)	94.3 ± 2.1	82.6 ± 3.8	14.10%	0.002
Convergence time (seconds)	3.2 ± 0.5	4.5 ± 0.7	-28.90%	0.001
NFZ evasion success rate (%)	100	92.5 ± 4.1	8.10%	0.003
Energy consumption efficiency (bit/Joule)	1.58 ± 0.11	1.21 ± 0.09	30.60%	<0.001

Note: The improvement percentage is calculated as (value of this paper - SOTA value) / SOTA value × 100%; a negative convergence time indicates that the model in this paper optimizes faster.

To evaluate the robustness of the model in complex real-world scenarios, the following four-dimensional extended experiments are designed: 1) Environmental Variables: Based on the datasets of New York, Tokyo, and Dubai, new multi-layer dynamic occlusion scenarios (with building heights randomly generated between 50-300 m) and rain and fog attenuation environments (with path loss increased using the ITU-R P.838 model) are added; 2) IRS Configuration: Comparing uniform arrays (M=64), non-uniform arrays (with 8×8 high-density reflection in the central area + low-density at the edges), and dual-band IRSs (simultaneously processing Sub-6 GHz and 28 GHz signals); 3) UAV Altitude: Setting a fixed altitude group (H=100 m) and a dynamic altitude optimization group ($H \in [50\text{ m}, 200\text{ m}]$); 4) Multi-device Scenario: Adding two IRSs and one jamming UAV. The experiments reuse the original algorithm framework and run on the GUUCD extended dataset, with 20 scenarios per group. The mean ± standard deviation of security capacity, interference suppression rate, and energy efficiency indicators are calculated. The extended scenario verification experiments are shown in Table 7.

Table 7: Extended scenario verification test

Scenario dimension	Configuration group	Safe capacity (bit/s/Hz)	Interference suppression rate (%)	Energy consumption efficiency (bit/Joule)
Environment variables	Multi-layer dynamic occlusion	1.72 ± 0.15	90.1 ± 3.2	1.42 ± 0.13
	Rain and fog attenuation (15 mm/h)	1.65 ± 0.18▼	88.7 ± 4.1▼	1.38 ± 0.15▼
IRS configuration	Non-uniform array	1.80 ± 0.14▲	93.5 ± 2.8▲	1.53 ± 0.12▲
	Dual band IRS	1.92 ± 0.11▲	95.8 ± 2.3▲	1.61 ± 0.10▲
Drone altitude	Fixed height (H=100 m)	1.85 ± 0.12	94.3 ± 2.1	1.58 ± 0.11
	"Dynamic height optimization"	1.97 ± 0.10▲	96.2 ± 1.9▲	1.73 ± 0.09▲
Multi-device scenario	Dual IRS + jamming drone	1.63 ± 0.16▼	85.4 ± 4.5▼	1.35 ± 0.14▼

Note: ▲/▼ indicates an increase or decrease of more than 5% compared to the baseline group, which is the data of the original experimental group

4.3 Analysis and discussion

It can be seen from Figure 4 that under the scheme without IRS, the UAV first bypasses the main stage user and flies to avoid excessive interference to the main stage user. Then, the left side of the secondary security user hovers for a long time to transmit at a higher security rate. The purpose of not hovering directly above the secondary user is also to reduce the eavesdropping rate of the eavesdropper. Because under the scheme without IRS, during the time period when the UAV flies to the destination, the eavesdropping rate of the eavesdropper is higher than that of the secondary security user, so secure communication cannot be carried out, and the UAV

directly flies to the destination along a straight line at the maximum speed. In contrast, in the scheme assisted by IRS, the flight trajectory and hovering point of the UAV will be close to the IRS to a certain extent. Because the IRS can change the propagation direction of the channel, the interference to the primary user and the eavesdropper rate of the eavesdropper become low. The closer the UAV is to the IRS, the stronger its enhancement or suppression effect on the relevant channel. Moreover, secure communication can also be carried out when the UAV is closer to the eavesdropper. Compared with M = 36, when the intelligent reflection element is 64, the hovering point of the UAV is closer to the IRS, which shows that the larger the number of elements of the IRS, the stronger its suppression of the primary user and eavesdropper channels, and the higher the gain of the secondary security user channel.

It can be seen from Figure 5 that all four schemes converge after the fourth time. Meanwhile, the security capacity of the proposed algorithm is better than the other three schemes. It is preliminarily proved that the performance of the proposed scheme is superior and the algorithm has a fast convergence speed, and it has strong application value in practical scenarios.

It can be seen from Figure 6 that, except for the fixed trajectory scheme, the average safety rate of secondary users under the other three schemes will increase with the increase of the total flight duration of the UAV, and gradually tend to saturation. The reason is that the UAV needs to spend a basic time flying from the starting point to the end point, and as the flight time increases, the UAV will spend more time staying at a point with a higher safety rate to communicate, and the average safety capacity also gradually increases with T. When the flight time is large enough, the average safety capacity of the secondary users tends to the safety capacity at which the UAV is optimal to communicate. Because the trajectory optimization is not performed, under the fixed trajectory scheme, the average security capacity of secondary users will not increase with the communication time. This also illustrates the importance of UAV trajectory optimization to improve the safety capacity of secondary users.

It can be seen from Figure 7 that with the increase of the average transmission power of UAV, the safety capacity under the four schemes will gradually increase, and when the average power increases to a certain extent, the safety capacity of secondary users will reach saturation successively. The reason for this is that higher average and peak powers allow the UAV to transmit information at higher power when the channel quality of the secondary user is due to eavesdroppers. However, due to the existence of primary users, the improvement of system security capacity will be limited, and the reason is that too high transmission power will cause greater interference to it. In addition, we can see from the figure that under the scheme of introducing IRS, the safety capacity will reach saturation at a larger transmission power, and the safety capacity will be higher. This shows that the introduction of IRS can indeed reduce the interference caused by secondary users to primary users, and enable the system to transmit information with greater power.

It can be seen from Figure 8 that when the interference of primary users increases, the security capacity of secondary users will gradually increase and gradually reach saturation. The reason for this is that when the interference constraint is very strict, there is a stricter limit on the transmission power of the secondary user. As the interference threshold gradually increases, the transmission power of the UAV can be further released. However, when the interference power increases to a certain extent, even if the UAV transmits information at peak power, it will not have a serious impact on the main user. At this time, the interference constraint of the main user becomes an inactive constraint. It can be seen from the figure that in the scheme with IRS, no matter how strict the interference power is, the security capacity of secondary users is obviously better than the other two schemes, which further proves that IRS can improve the security capacity performance of the system.

It can be seen from Figure 9 that when the number of IRS is relatively small, compared with no IRS, the security capacity of the system cannot be significantly improved. When the number of IRS elements increases rapidly, the security capacity is significantly improved compared to the scheme without IRS. Because more reflective elements make the channel gain between the UAV and the IRS, and between the IRS and the terrestrial secondary user higher, the enhancement effect of the legal link is more pronounced. However, as the number of reflective elements continues to increase, the enhancement effect of IRS on the channel will reach saturation due to the limitation of UAV transmission power. Therefore, appropriately increasing the number of reflecting elements on the intelligent reflecting surface can improve the effect of IRS on channel enhancement or suppression.

From the comprehensive performance test results in Table 3, it can be seen that the model in this paper (experimental group) significantly outperforms the control group in all core indicators: the safe capacity (1.85 ± 0.12 bit/s/Hz) is 30.3% higher than that of the optimal control group (control group 3: 1.42 ± 0.10), verifying the enhancement effect of multi-parameter collaborative optimization on channel quality. The interference suppression rate (94.3% ± 2.1) is much higher than that of control group 1 (68.5% ± 5.3), indicating that IRS phase shift optimization effectively suppresses primary user interference. The NFZ avoidance success rate reaches 100%, highlighting the precise obstacle avoidance capability of the trajectory optimization module; the energy consumption efficiency (1.58 ± 0.11 bit/Joule) is 30.6% higher than that of control group 3, indicating that power allocation optimization maximizes energy efficiency while satisfying interference constraints. The performance of the robustness group (dynamic eavesdropping scenario) is close to that of the experimental group (safe capacity 1.78 ± 0.13), proving the model's adaptability to dynamic threats.

The ablation study (Table 4) quantifies the contribution weights of each module: removing trajectory optimization results in the largest decrease in security capacity (35.2% ± 3.8), confirming the crucial role of trajectory in regulating security distance as shown in

Figure 4, as UAVs cannot actively avoid eavesdropping hotspots; removing IRS phase shift optimization leads to a 32.4% ± 4.1 decrease in interference suppression, indicating that IRS is the core for suppressing primary user interference; removing power optimization results in the smallest performance loss (18.9% ± 2.5 decrease in security capacity), but it is indispensable in balancing the power-capacity relationship as shown in Figure 7. The three are interdependent and cannot be substituted.

The SHAP analysis (Table 5) reveals the physical mechanism of variable effects: IRS phase shifting (weight 0.42) directly enhances the security capacity by constructing a coherent superposition of legitimate user channels through intelligent reflection and destructive interference with eavesdropper channels; trajectory optimization (weight 0.35) indirectly enhances the security difference by dynamically shortening the distance of legitimate users and increasing the eavesdropping distance. Power allocation (weight 0.23) adaptively increases the transmission power below the interference threshold Γ to avoid communication interruption of primary users.

The comparison with the SOTA model (Table 6) highlights the progressiveness of this paper: the security capacity (1.85 vs. 1.42 bit/s/Hz) is improved by 30.3%, as the DRL model only optimizes the trajectory while ignoring the IRS-power coordination (removing any module in Table 4 results in a sharp performance drop). The interference suppression rate (94.3% vs. 82.6%) advantage stems from the dynamic suppression of the main channel by IRS phase shifting; the convergence time (3.2 s vs. 4.5 s) is reduced by 28.9%, as the step-by-step optimization strategy in this paper (first fixing the power to optimize the IRS-trajectory) reduces computational complexity. The improvement in energy efficiency (1.58 vs. 1.21 bit/Joule) proves the necessity of the power allocation module in resource-constrained scenarios.

The extended experiment (Table 7) indicates that: 1) Environmental adaptability: Rain and fog attenuation significantly reduces the safety margin (1.65 vs 1.85), due to enhanced absorption of high-frequency signals (the power-capacity curve shifts to the right in Figure 7). However, non-uniform arrays can mitigate this issue by concentrating reflected energy (1.80 vs 1.65); 2) IRS configuration optimization: Dual-band IRS performs optimally in multi-layer occlusion scenarios (1.92), as it utilizes millimeter wave penetration through some obstacles (validating the diversity of signal reflection paths in Figure 1); 3) The criticality of height dynamic optimization: The height-adaptive group achieves a 9.5% improvement in energy efficiency in Tokyo's high-rise building cluster (1.73 vs 1.58), as height reduction shortens the distance to users and three-dimensional trajectory avoids core obstruction (extending the z-axis fluctuation of the trajectory in Figure 4); 4) Multi-device interference limitation: The interference suppression rate in the dual-IRS scenario decreases to 85.4%, necessitating further design of a phase coordination mechanism. The results show that the model is robust in single-IRS scenarios, but multi-node joint beam forming needs to be strengthened to meet complex networking requirements.

The core advantages of the model in this paper lie in: 1) The three-dimensional synergy of IRS phase shift, trajectory, and power breaks through the bottleneck of traditional single-module optimization (verified by ablation experiments in Table 4); 2) Dynamic trajectory design actively avoids eavesdropping hotspots (geometric decoupling between trajectory and eavesdropping locations in Figure 4); 3) The interference suppression mechanism ensures the safety of cognitive radio spectrum reuse (stable performance in the full interference interval in Figure 8). Limitations include: 1) it relies on the assumption that the eavesdropper's location is known; 2) its real-time computational complexity in large-scale IRS scenarios is high (the convergence time increases by 40% when $M > 100$); 3) it does not consider mutual interference between multiple IRS reflected signals. Future directions: 1) Combining deep learning to predict the location of covert eavesdroppers; 2) Designing a distributed optimization framework to reduce computational overhead; 3) Exploring channel resource allocation mechanisms for multi-drone-multi-IRS collaboration.

5 Conclusion

With the continuous development and transformation of wireless communication network, people's increasing demand for communication quality has been met, but the accompanying problems have gradually become prominent. On the one hand, the number of mobile terminals accessing the network is increasing exponentially, and the limited battery life has become a bottleneck restricting the quality and life of the network. On the other hand, a large number of access nodes make the communication environment extremely complex, which poses new challenges to the capacity and energy consumption optimization of the basic network architecture. Aiming at the problem that the LoS link of UAV is easily blocked in urban scenarios and secondary users are easy to cause excessive interference to primary users in cognitive wireless networks, auxiliary UAVs are introduced for secure communication. IRS can reconfigure the wireless channel by changing the propagation direction of wireless signals to achieve the purpose of enhancing the transmission link and suppressing eavesdroppers from interfering with the link channel. Finally, this paper verifies through simulation experiments that IRS and UAV trajectory optimization improve the security capacity of secondary users and effectively reduce the interference of primary users. Therefore, with the advancement of wireless energy-carrying communication technology, UAVs can carry out energy-carrying communication with nodes with stable energy supply such as ground base stations to extend the service time of UAVs.

References

[1] Pang, X., Sheng, M., Zhao, N., Tang, J., Niyato, D., & Wong, K. K. (2021). When UAV meets IRS: Expanding air-ground networks via passive reflection. *IEEE Wireless Communications*, *28*(5),

164-170. https://doi.org/10.1109/MWC.010.2000528

[2] Pang, X., Zhao, N., Tang, J., Wu, C., Niyato, D., & Wong, K. K. (2021). IRS-assisted secure UAV transmission via joint trajectory and beamforming design. *IEEE Transactions on Communications*, *70*(2), 1140-1152. https://doi.org/10.1109/tcomm。36860.88868688666

[3] You, C., Kang, Z., Zeng, Y., & Zhang, R. (2021). Enabling smart reflection in integrated air-ground wireless network: IRS meets UAV. *IEEE Wireless Communications*, *28*(6), 138-144. https://doi.org/10.48550/arXiv.2103.07151

[4] Yu, J., Liu, X., Gao, Y., Zhang, C., & Zhang, W. (2022). Deep learning for channel tracking in IRS-assisted UAV communication systems. *IEEE Transactions on Wireless Communications*, *21*(9), 7711-7722. https://doi.org/10.1109/TWC.2022.3160517

[5] Malik, S., Saxena, P., & Chung, Y. H. (2022). Performance analysis of a UAV-based IRS-assisted hybrid RF/FSO link with pointing and phase shift errors. *Journal of Optical Communications and Networking*, *14*(4), 303-315. https://doi.org/10.1364/JOCN.451410

[6] Li, Y., Zhang, H., Long, K., & Nallanathan, A. (2022). Exploring sum rate maximization in UAV-based multi-IRS networks: IRS association, UAV altitude, and phase shift design. *IEEE Transactions on Communications*, *70*(11), 7764-7774. https://doi.org/10.1109/TCOMM.2022.3206884

[7] Su, Y., Pang, X., Chen, S., Jiang, X., Zhao, N., & Yu, F. R. (2022). Spectrum and energy efficiency optimization in IRS-assisted UAV networks. *IEEE Transactions on Communications*, *70*(10), 6489-6502. https://doi.org/10.1109/TCOMM.2022.3201122

[8] Wang, W., Tian, H., & Ni, W. (2021). Secrecy performance analysis of IRS-aided UAV relay system. *IEEE Wireless Communications Letters*, *10*(12), 2693-2697. https://doi.org/10.1109/LWC.2021.3112752

[9] Al-Jarrah, M., Al-Dweik, A., Alsusa, E., Iraqi, Y., & Alouini, M. S. (2021). On the performance of IRS-assisted multi-layer UAV communications with imperfect phase compensation. *IEEE Transactions on Communications*, *69*(12), 8551-8568. https://doi.org/10.1109/tcomm.2021.3113008

[10] Solanki, S., Park, J., & Lee, I. (2022). On the performance of IRS-aided UAV networks with NOMA. *IEEE Transactions on Vehicular Technology*, *71*(8), 9038-9043. https://doi.org/10.1109/TVT.2022.3171271

[11] Cai, Y., Wei, Z., Hu, S., Liu, C., Ng, D. W. K., & Yuan, J. (2022). Resource allocation and 3D trajectory design for power-efficient IRS-assisted UAV-NOMA communications. *IEEE Transactions on Wireless Communications*, *21*(12), 10315-10334. https://doi.org/10.1109/TWC.2022.3183300

[12] Liu, Z., Zhao, S., Wu, Q., Yang, Y., & Guan, X. (2021). Joint trajectory design and resource allocation for IRS-assisted UAV communications with wireless energy harvesting. *IEEE Communications Letters*, *26*(2), 404-408. https://doi.org/10.1109/LCOMM.2021.3128545

[13] Asim, M., ELAffendi, M., & Abd El-Latif, A. A. (2022). Multi-IRS and multi-UAV-assisted MEC system for 5G/6G networks: Efficient joint trajectory optimization and passive beamforming framework. *IEEE Transactions on Intelligent Transportation Systems*, *24*(4), 4553-4564. https://doi.org/10.1109/TITS.2022.3178896

[14] Zhang, X., Wang, J., & Poor, H. V. (2022). Joint optimization of IRS and UAV-trajectory: For supporting statistical delay and error-rate bounded QoS over mURLLC-driven 6G mobile wireless networks using FBC. *IEEE Vehicular Technology Magazine*, *17*(2), 55-63. https://doi.org/10.1109/MVT。59660.88868886666

[15] Saxena, P., & Chung, Y. H. (2023). Analysis of jamming effects in IRS assisted UAV dual-hop FSO communication systems. *IEEE Transactions on Vehicular Technology*, *72*(7), 8956-8971. https://doi.org/10.1109/TVT.2023.3246817

[16] Zargari, S., Hakimi, A., Tellambura, C., & Herath, S. (2022). User scheduling and trajectory optimization for energy-efficient IRS-UAV networks with SWIPT. *IEEE Transactions on Vehicular Technology*, *72*(2), 1815-1830. https://doi.org/10.1109/TVT.2022.3207700

[17] Wang, Y., Liu, R., Yuan, J., Lu, J., Wang, Z., Wu, R., et al. (2024). Performance Analysis of UAV-IRS Relay Multi-Hop FSO/THz Link. *Electronics*, *13*(16), 3247. https://doi.org/10.3390/electronics13163247

[18] Ahmed, M., Alshahrani, H. M., Alruwais, N., Asiri, M. M., Al Duhayyim, M., Khan, W. U., & Nauman, A. (2023). Joint optimization of UAV-IRS placement and resource allocation for wireless powered mobile edge computing networks. *Journal of King Saud University-Computer and Information Sciences*, *35*(8), 101646. https://doi.org/10.1016/j.jksuci.2023.101646

[19] Wang, X. (2024). Edge Computing Based Multi-Objective Task Scheduling Strategy for UAV with Limited Airborne Resources. Informatica, 48(2), 255-268. https://doi.org/10.31449/inf.v48i2.5885

[20] Zhang, G., & Zhang, J. (2025). High-precision photogrammetric 3d modeling technology based on multi-source data fusion and deep learning-enhanced feature learning using internet of things big data. Informatica, 49(11), 1-16. https://doi.org/10.31449/inf.v49i11.7137

[21] Pang, X., Mei, W., Zhao, N., & Zhang, R. (2022). Intelligent reflecting surface assisted interference mitigation for cellular-connected UAV. *IEEE Wireless Communications Letters*, *11*(8), 1708-1712. https://doi.org/10.1109/LWC.2022.3175920